

# Synchronized Andreev Transmission in Chains of SNS Junctions

N. M. Chtchelkatchev<sup>1,2,3</sup>, T. I. Baturina<sup>3,4</sup>, A. Glatz<sup>3</sup>, and V. M. Vinokur<sup>3</sup>

<sup>1</sup> Institute for High Pressure Physics, Russian Academy of Sciences, Troitsk 142190, Moscow region, Russia

<sup>2</sup> L.D. Landau Institute for Theoretical Physics, Russian Academy of Sciences, Akademika Semenova av. 1-A, Chernogolovka 142432, Moscow Region, Russia

<sup>3</sup> Materials Science Division, Argonne National Laboratory, Argonne, Illinois 60439, USA [vinokour@anl.gov](mailto:vinokour@anl.gov)

<sup>4</sup> Institute of Semiconductor Physics, 13 Lavrentjev Avenue, Novosibirsk 630090, Russia

**Abstract.** We construct a nonequilibrium theory for the charge transfer through a diffusive array of alternating normal (N) and superconducting (S) islands comprising an SNSNS junction, with the size of the central S-island being smaller than the energy relaxation length. We demonstrate that in the nonequilibrium regime the central island acts as Andreev retransmitter with the Andreev conversions at both NS interfaces of the central island correlated via over-the-gap transmission and Andreev reflection. This results in a synchronized transmission at certain resonant voltages which can be experimentally observed as a sequence of spikes in the differential conductivity.

## 1.1 Introduction

An array of alternating superconductor (S) - normal metal (N) islands is a fundamental laboratory representing a wealth of physical systems ranging from Josephson junction networks and layered high temperature superconductors to disordered superconducting films in the vicinity of the superconductor-insulator transition. Electronic transport in these systems is mediated by Andreev conversion of a supercurrent into a current of quasiparticles and vice versa at interfaces between the superconducting and normal regions [1]. A fascinating phenomenon benchmarking this mechanism is the enhancement of the conductivity observed in a single SNS junction at matching voltages constituting an integer ( $m$ ) fraction of the superconducting gap,  $V = 2\Delta/(em)$  [2–11] due to the effect of multiple Andreev reflection (MAR) [12–14]. The current-voltage characteristics of diffusive SNS junctions were discussed in great detail

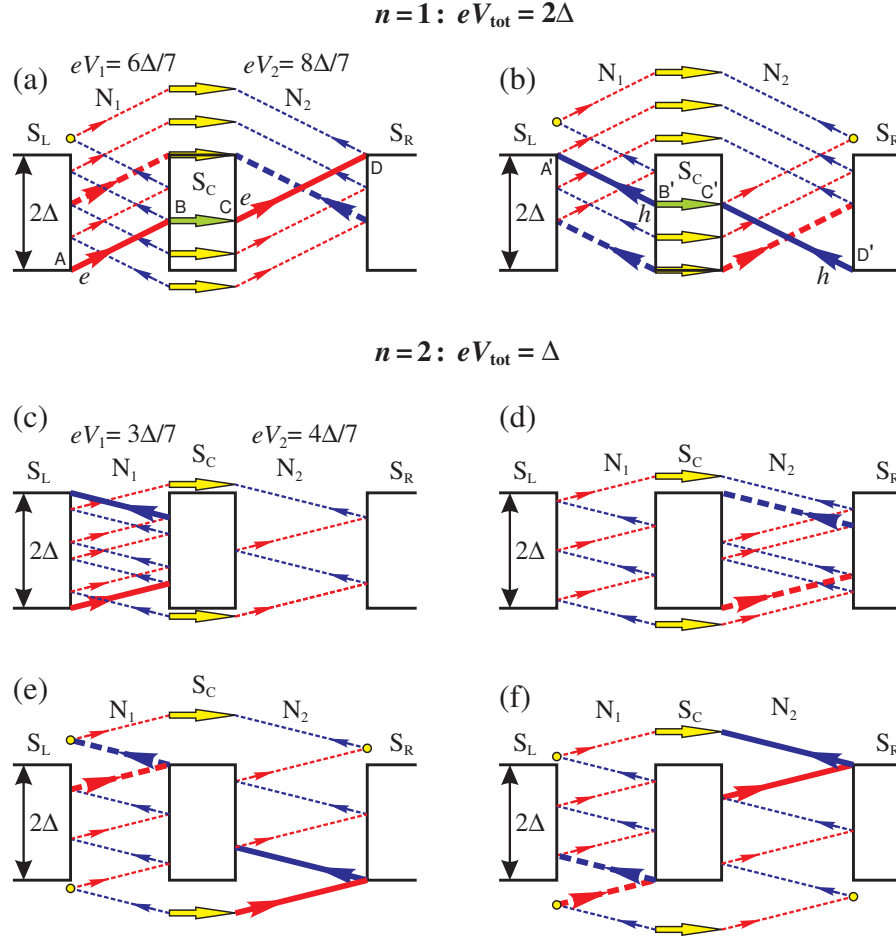


**Fig. 1.1.** Diagrams of the SAT processes for the first,  $n = 1$ , (a)-(b), and second,  $n = 2$  (c)-(f), subharmonics of the resonant singularities in  $dI/dV$  described by Eq. (1.1) for the SNSNS junction with the normal resistances ratio  $R_1/R_2 = 3/4$  (depicted through  $3/4$  ratio of the respective lengths of the normal regions). The thick solid lines represent the quasiparticle paths starting and/or ending at the points of singularity in the density of states at energies  $\varepsilon = \pm\Delta$  at the electrodes  $S_L$  and  $S_R$ . The dashed solid lines show paths starting and/or ending at the edges of the gap of the central island  $S_C$ . The circle denotes the over-the-gap Andreev reflections at the electrodes. The paths ABCD [panel (a)] and D'C'B'A' [panel (b)] correspond to the electron- and hole trajectories, respectively. Synchronization of the energies of the incident and emitted quasiparticles at points B and C (B' and C') is shown by arrows. SAT is realized by trajectories passing through the singular points  $\varepsilon = \pm\Delta$  of the central island  $S_C$  and including over-the-gap transmissions and Andreev reflections. Trajectories synchronizing other transmissions across  $S_C$  and those of higher orders are not shown. Note, that voltage drops  $eV_1 = 6\Delta/7$  and  $eV_2 = 8\Delta/7$  [panels (a)-(b)] ( $eV_1 = 3\Delta/7$  and  $eV_2 = 4\Delta/7$  [panels (c)-(f)]) are not MAR matching voltages of individual  $S_L N_1 S_C$  or  $S_C N_2 S_R$  parts.

in Refs. [15,16]. Further developments were obliged to studies of large arrays comprised of many SNS junctions [17–21]. Experimental results, especially those obtained on the multiconnected arrays [17,18,21], indicated clearly that singularities in transport characteristics cannot be explained by MARs at individual SNS junctions only and that there is evidently a certain coherence of the Andreev processes that occur at different NS interfaces. These findings call for a comprehensive theory of transport in large SNS arrays.

In this article we develop a nonequilibrium theory of electronic transport in a series of two diffusive SNS junctions, i.e. an SNSNS junction and derive the corresponding current-voltage characteristics. We demonstrate that splitting the normal part of the SNS junction into two normal islands that have, in general, different resistances and are coupled via a small superconducting granule,  $S_C$  leads to the nontrivial physics and emergence of a new distinct resonant mechanism for the current transfer: *the Synchronized Andreev Transmission (SAT)*. The main component of our consideration is a *nonequilibrium circuit theory* of the charge transfer across  $S_C$ . [The symmetric case with the equal resistances of the normal parts was discussed in detail in [22]. Unfortunately the technique developed there does not allow straightforward generalization onto a nonsymmetric case.]

In the SAT regime the processes of Andreev conversion at the boundaries of the central superconducting island are correlated: as a quasiparticle with the energy  $\varepsilon$  hits one  $NS_C$  interface, a quasiparticle with the same energy emerges from the other  $S_CN$  interface and enters the bulk of the normal island (and vice versa, see Fig. 1). This energy synchronization is achieved via over-the-gap Andreev processes [19], which couple MARs occurring within the each of the normal islands and make the quasiparticle distribution at the central island essentially nonequilibrium. Effectiveness of the synchronization is controlled by the value of the energy relaxation lengths of both, the quasiparticles crossing  $S_C$  with energies above  $\Delta$ , and the quasiparticles experiencing MAR in the normal parts. The SAT processes result in spikes in the differential conductivity of the SNSNS circuit, which appear at resonant values of the *total* applied voltage  $V_{\text{tot}}$  defined by the condition

$$V_{\text{tot}} = \frac{2\Delta}{en} \quad (1.1)$$

with integer  $n$ , irrespectively of the details of the distribution of the partial voltages at the two normal islands.

The article is organized as follows. In the Section 1.2 we define the system, a diffusive SNSNS junction which will be a subject of our study. Section 1.3 is devoted to introduction and description of the employed theoretical tools: the electronic transport of the system in the resistive state is given by the Larkin-Ovchinnikov equation in a form of matrix equations for the Green's functions taken in Keldysh representation. In Sections 1.4-1.8 we construct an equivalent circuit theory for an SNSNS junction resulting in the recurrent relations for the spectral current flow in the energy space. In Section 1.9 we present the

original numerical method enabling us to solve the recurrent relations for the spectral current and obtain the  $I$ - $V$  characteristics for the SNSNS junction. The obtained results are discussed in Section 1.10, where we demonstrate, in particular, that the SAT-induced features become dominant in large arrays consisting of many SNS junctions.

## 1.2 The system

We consider charge transfer across an  $S_L N_1 S_C N_2 S_R$  junction, where  $S_L$ ,  $S_C$ , and  $S_R$  are mesoscopic superconductors with the identical gap  $\Delta$ ; the ‘edge’ superconducting granules  $S_L$  and  $S_R$  play the role of electrodes, and  $S_C$  is the central island separating the two normal parts with, in general, different normal resistances. We discuss the common experimental situation of a diffusive regime where the most of the energy scales are smaller than  $\hbar/\tau$ , where  $\tau$  is the impurity scattering time. We assume the size,  $L_C$ , of the central island to be much larger than the superconducting coherence length  $\xi$ , hence processes of subgap elastic cotunneling and/or direct Andreev tunneling [23] do not contribute much to the charge transfer. In general, this condition ensures that  $L_C$  is large enough so that charges do not accumulate in the central island and Coulomb blockade effects are irrelevant for the quasiparticle transport. At the same time  $L_C$  is assumed to be less than the charge imbalance length, such that we can neglect the coordinate dependence of the quasiparticle distribution functions across the island  $S_C$ . Additionally, the condition  $\ell_\varepsilon \gg L_C$ , where  $\ell_\varepsilon$  is the energy relaxation length, implies that quasiparticles with energies  $\varepsilon > \Delta$  traverse the central superconducting island  $S_C$  without any noticeable loss of energy. The normal parts  $N_1$  and  $N_2$  are the diffusive normal metals of length  $L_{1,2} > \xi$ , and  $L_{1,2} > L_T$ ,  $L_T = \sqrt{\hbar D_N / \varepsilon}$ , where  $D_N$  is the diffusion coefficient in the normal metal. We assume the Thouless energy,  $E_{Th} = \hbar D_N / L_{1,2}^2$ , to be small,  $E_{Th} \ll \Delta$ , and not to exceed the characteristic voltage drops,  $E_{Th} < eV_{1,2}$ . If these conditions that define the so called incoherent regime [15] are met, the Josephson coupling between the superconducting islands is suppressed. And, finally, we let the energy relaxation length in the normal parts  $N_1$  and  $N_2$  be much larger than their sizes, so that quasiparticles may experience many incoherent Andreev reflections inside the normal regions.

## 1.3 Theoretical formalism

The current transfer across the SNSNS junction is described by quasiclassical Larkin-Ovchinnikov (LO) equations for the dirty limit [24, 25]:

$$-i[\check{H}_{\text{eff}^\circ}, \check{\mathbf{G}}] = \nabla \check{\mathbf{J}}, \quad \check{\mathbf{J}} \cdot \mathbf{n} = \frac{1}{2\sigma_s R} [\check{G}_s, \check{G}_N], \quad (1.2)$$

where  $\tilde{H}_{\text{eff}} = \hat{1}(i\hat{\sigma}_z\partial_t - \varphi\hat{\sigma}_0 + \hat{\Delta})$ ,  $\tilde{\mathbf{J}} = D\tilde{\mathbf{G}} \circ \nabla\tilde{\mathbf{G}}$  is the matrix current, the subscripts “S” and “N” denote the superconducting and normal materials, respectively, “o” stands for the time-convolution,  $\hat{\sigma}_i$  ( $i=x,y,z$ ) are the Pauli matrices, operating in the Nambu space of  $2 \times 2$  matrices denoted by ‘hats’,  $\hat{\Delta} = i\hat{\sigma}_x \text{Im } \Delta + i\hat{\sigma}_y \text{Re } \Delta$ , and  $R$  is the resistance of an NS interface. The diffusion coefficient  $D$  assumes the value  $D_N$  in the normal metal and the value  $D_S$  in the superconductor, and  $\varphi$  is the electrical potential which we calculate self-consistently. The unit vector  $\mathbf{n}$  is normal to the NS interface and is assumed to be directed from N to S. The momentum averaged Green’s functions  $\tilde{\mathbf{G}}(\mathbf{r}, t, t')$  are  $2 \times 2$  supermatrices in a Keldysh space. Each element of the Keldysh matrix, labelled with a hat sign, is, in its turn, a  $2 \times 2$  matrix in the electron-hole space:

$$\tilde{\mathbf{G}} = \begin{pmatrix} \hat{G}^R & \hat{G}^K \\ 0 & \hat{G}^A \end{pmatrix}; \quad \hat{G}^{R(A)} = \begin{pmatrix} \mathcal{G}^{R(A)} & \mathcal{F}^{R(A)} \\ \tilde{\mathcal{F}}^{R(A)} & \tilde{\mathcal{G}}^{R(A)} \end{pmatrix}, \quad (1.3)$$

$\mathbf{r}$  is the spatial position,  $t$  and  $t'$  are the two time arguments. The Keldysh component of the Green’s function is parametrized as [24]:  $\hat{G}^K = \hat{G}^R \circ \hat{f} - \hat{f} \circ \hat{G}^A$ , where  $\hat{f}$  is the distribution function matrix, diagonal in Nambu space,  $\hat{f} \equiv \text{diag}[1 - 2n_e, 1 - 2n_h]$ ,  $n_{e(h)}$  is the electron (hole) distribution function. In equilibrium  $n_{e(h)}$  becomes the Fermi function. And, finally, the Green’s function satisfies the normalization condition  $\tilde{\mathbf{G}}^2 = \hat{1}$ .

The edge conditions closing Eqs. (1.2) are given by the expressions for the Green’s functions in the bulk of the left (L) and right (R) superconducting leads:

$$\tilde{\mathbf{G}}_{L(R)}(t, t') = e^{-i\mu_{L(R)}t\hat{\tau}_3/\hbar} \tilde{\mathbf{G}}_0(t - t') e^{i\mu_{L(R)}t'\hat{\tau}_3/\hbar},$$

the chemical potentials are  $\mu_L = 0$  and  $\mu_R = eV$ . Here,  $\tilde{\mathbf{G}}_0(t)$  is the equilibrium bulk BCS Green’s function.

The current density is expressed through the Keldysh component of  $\tilde{\mathbf{J}}$  as

$$\mathcal{I}(t, \mathbf{r}) = \frac{\pi\sigma_N}{4} \text{Tr } \hat{\sigma}_z j^K(t, t; \mathbf{r}) = \frac{1}{2} \int d\varepsilon [I_e(\varepsilon) + I_h(\varepsilon)], \quad (1.4)$$

where the spectral currents  $I_e$  and  $I_h$  representing the electron and hole quasi-particle currents, respectively, are the time Wigner-transforms of top- and bottom diagonal elements of the matrix current  $\tilde{\mathbf{J}}^{(K)}$ .

On the normal side of the superconductor-normal metal interface, the Keldysh component of Eqs. (1.2) yield the conservation conditions:

$$\nabla I_{e(h)} = 0, \quad (1.5)$$

$$I_e(\varepsilon) = \sigma_N \{D_p(\varepsilon + u) \nabla n_e(\varepsilon) - D_m(\varepsilon + u) \nabla n_h(\varepsilon + 2u)\}, \quad (1.6)$$

$$I_h(\varepsilon) = \sigma_N \{D_p(\varepsilon - u) \nabla n_h(\varepsilon) - D_m(\varepsilon - u) \nabla n_e(\varepsilon - 2u)\}, \quad (1.7)$$

where  $u$  is the electrical potential of the adjacent superconductor,  $D_{p(m)} = (D_- \pm D_+)/2$ ,

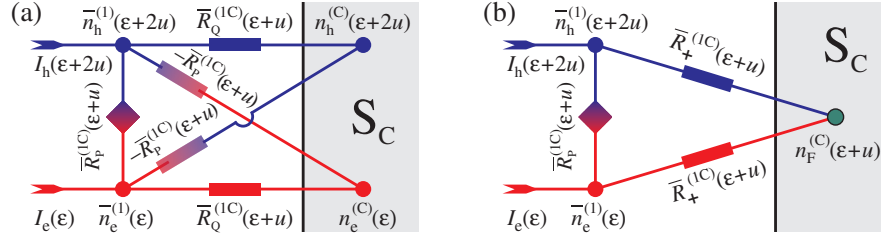


**Fig. 1.2.** Effective circuit for the boundary between the normal metal and the superconductor. Kirchhoff laws where the role of the potential in the nodes is taken by the electron- and hole distribution functions give the boundary conditions for the LO equations. (a) A general nonequilibrium case. (b) Equivalent circuit for an equilibrium case where quasiparticle distribution functions in the superconductor are the Fermi-functions,  $n_F$ , then  $n_e(\epsilon) = n_F(\epsilon + u) = n_h(\epsilon + 2u)$ , used in [15]. The superconductor electrical potential at the boundary is equal to  $u$ .

$$D_+(\epsilon) = \frac{1}{4} \text{Tr}[\hat{1} - \hat{G}^R(\epsilon) \hat{G}^A(\epsilon)],$$

$$D_-(\epsilon) = \frac{1}{4} \text{Tr}[\hat{1} - \sigma^z \hat{G}^R(\epsilon) \sigma^z \hat{G}^A(\epsilon)],$$
(1.8)

and the trace is taken over components in the Nambu-space. In the bulk of a normal metal,  $\hat{G}^{R(A)}(\epsilon) \rightarrow \pm \sigma_z$  and  $D_+ \approx D_- \approx 1$ , so  $I_e = \sigma_N \nabla n_e$  and  $I_h = \sigma_N \nabla n_h$ .

#### 1.4 Circuit representation of the boundary conditions

We start the construction of the circuit theory with the corresponding formulation of the boundary conditions for the distribution functions at the interface between the normal parts and the central superconducting island. We consider a stationary situation where the applied voltage does not depend on time. Then the Green's functions can be parameterized near an NS interface as follows:

$$[\hat{G}^R]_j(\epsilon, \epsilon') = \hat{\sigma}_z \delta_{\epsilon-\epsilon'} \cosh \theta_j(\epsilon) +$$

$$\hat{\sigma}_+ \delta_{\epsilon-\epsilon'+2u} \sinh \theta_j(\epsilon) - \hat{\sigma}_- \delta_{\epsilon-\epsilon'-2u} \sinh \theta_j(\epsilon),$$

$$G^A = -\hat{\sigma}_z (G^R)^\dagger \hat{\sigma}_z,$$
(1.9)

where  $\hat{\sigma}_\pm = \hat{\sigma}_x \pm i\hat{\sigma}_y$ ,  $j=S, N$ , and  $u$  is the electrochemical potential. The effective diffusion coefficients are correspondingly  $D_+ = \cos^2 \text{Im} \theta$  and  $D_- = \cosh^2 \text{Re} \theta$ . When deriving Eq.(1.9), we have used the condition that the Josephson coupling between the superconducting islands in the junction is suppressed. The proximity effect results in an additional term in Eq.(1.9) proportional to  $\delta(\epsilon - \epsilon' - 2(u' - u))$ , where  $u'$  is the potential of the adjacent superconductor involved.

Taking the Keldysh component of the boundary term in Eq. (1.2) we derive the boundary conditions for the currents  $I_{e(h)}$  at the NS interface, which assume the form of Kirchhoff's laws for the circuit shown in Fig. 1.2(a). The electron and hole distribution functions take the role of voltages at the nodes. The equation for an electronic spectral current flowing into the lower left corner node:

$$I_e(\varepsilon) = \frac{n_e^{(c)}(\varepsilon) - n_e^{(1)}(\varepsilon)}{R_Q^{(1c)}(\varepsilon + u)} + \frac{n_h^{(c)}(\varepsilon + 2u) - n_e^{(1)}(\varepsilon)}{[-R_P^{(1c)}(\varepsilon + u)]} + \frac{n_h^{(1)}(\varepsilon + 2u) - n_e^{(1)}(\varepsilon)}{R_P^{(1c)}(\varepsilon + u)}. \quad (1.10)$$

The equation for the hole current going into the top left node of the circuit of the Fig. 1.2(a) is easily obtained analogously to (1.10) with the aid of the additional transformation  $\varepsilon \rightarrow \varepsilon - 2u$  i.e. by shifting all the energies over  $-2u$ :

$$I_h(\varepsilon) = \frac{n_h^{(c)}(\varepsilon) - n_h^{(1)}(\varepsilon)}{R_Q^{(1c)}(\varepsilon - u)} + \frac{n_e^{(c)}(\varepsilon - 2u) - n_h^{(1)}(\varepsilon)}{[-R_P^{(1c)}(\varepsilon - u)]} + \frac{n_e^{(1)}(\varepsilon - 2u) - n_h^{(1)}(\varepsilon)}{R_P^{(1c)}(\varepsilon - u)}. \quad (1.11)$$

In an equilibrium the quasiparticles in the superconductor follow the Fermi distribution, then  $n_e^{(c)}(\varepsilon) = n_F(\varepsilon + u) = n_h^{(c)}(\varepsilon + 2u)$  and Eqs.(1.10)-(1.11) reduce to

$$I_e(\varepsilon) = \frac{n_F(\varepsilon - u) - n_e^{(1)}(\varepsilon)}{R_+^{(1c)}(\varepsilon + u)} + \frac{n_h^{(1)}(\varepsilon + 2u) - n_e^{(1)}(\varepsilon)}{R_P^{(1c)}(\varepsilon + u)}, \quad (1.12)$$

where the interjacent resistances are defined as  $R_{Q(P)}^{-1}(\varepsilon) = \{R_-^{-1}(\varepsilon) \pm \bar{R}_+^{-1}(\varepsilon)\}/2$ ; here  $1/R_{\pm}(\varepsilon) = [N_2 N_1 \mp M_2^{\pm} M_1^{\pm}]/R$ ,  $N_j(\varepsilon) = \text{Re} \cosh \theta_j$ ,  $M_j^+(\varepsilon) + i M_j^-(\varepsilon) = \sin \theta_j$  and  $j = 1, 2$  labels the different sides of the interface.

The circuit representation of Eq.(1.12) is shown in Fig. 1.2(b). This is the boundary conditions and the corresponding circuit used in Ref. [15].

## 1.5 Conductance renormalization procedure

We consider the normal metal between the left superconducting lead  $S_L$  and the superconducting island,  $S_C$ , see Fig. 1.3. The boundary conditions, Eqs.(1.10)-(1.11), relate electron and hole distribution functions at the right NS and left NS interfaces. Below we relate electron and hole distribution functions at  $x = 0$  and  $x = d$  building the effective circuit, where  $d$  is the length

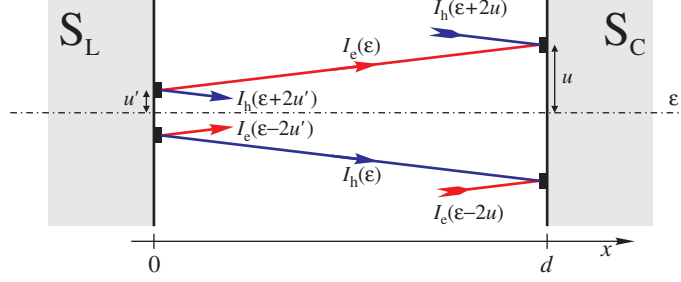


**Fig. 1.3.** Illustration of the spectral currents flow in the normal metal [white area] surrounded by the superconductors [grey area]. The black boxes at the interfaces encode the boundary conditions picture like it is shown in Fig.1.2.

of the normal layer. At the first step we neglect the proximity effect change of the junction resistance and take  $D_{\pm} = 1$  everywhere in the normal layer. Then,  $I_{e(h)} = \sigma_1 \nabla n_{e(h)}$ ,  $\Delta n_{e(h)} = 0$  and therefore

$$I_{e(h)}(\varepsilon) = [n_{e(h)}(d, \varepsilon) - n_{e(h)}(x = 0, \varepsilon)]/R_1, \quad (1.13)$$

where  $R_1 = \sigma_1/d$  is the normal resistance of the  $N_1$ -layer. Eq.(1.13) resembles the Ohm law for the resistor  $R_1$ , but where the role of the voltages play the distribution functions at the ends of the resistor. Eq.(1.13) is approximate because it neglects the proximity renormalization of the normal layer conductivity [26]. It was shown in Ref. [15] for a SNS junction that the replacement of  $n_{e(h)}(x = \{0, d\})$  by the properly chosen proximity renormalized distribution functions makes Eq.(1.13) accurate. We show below that this idea is applicable when electron and hole distribution functions in the superconductors essentially deviate from the Fermi functions and when the electron and hole currents can not be in general related by a shift of the energy like in SNS junction.

At the left NS-interface the spectral currents,  $I_e(\varepsilon)$  and  $I_h(\varepsilon + 2u)$  are related by the Andreev process, see Fig.1.2a. It follows from Eqs.(1.5)-(1.7) that the combination of the quasiparticle currents,  $I_{\pm}^{(1C)}(\varepsilon) = I_e(\varepsilon) \pm I_h(\varepsilon + 2u) = \sigma_1 D_{\pm}^{(1C)}(\varepsilon + u) \nabla n_{\pm}^{(1C)}(\varepsilon + u)$ , conserve in the normal metal:  $\nabla I_{\pm}^{(1C)} = 0$ . Integrating the last equation over  $x$  we get,

$$I_{\pm}^{(1C)} \int_0^d \frac{dx}{D_{\pm}^{(1C)}(x)} = \sigma_1 [n_{\pm}(d) - n_{\pm}(x)], \quad (1.14)$$

where  $n_{\pm}^{(1C)}(\varepsilon) = n_e(\varepsilon) \pm n_h(\varepsilon + 2u)$ . Eq.(1.14) can be equivalently rewritten:

$$I_{\pm}^{(1C)}(d - x) = \sigma_1 [\bar{n}_{\pm}^{(1C)}(d) - n_{\pm}^{(1C)}(x)], \quad (1.15)$$

$$\bar{n}_{\pm}^{(1C)}(d) \equiv n_{\pm}^{(1C)}(d) - m_{\pm}^{(1C)} I_{\pm}^{(1C)}(\varepsilon + u), \quad (1.16)$$

where



$$m_{\pm}^{(1C)} = \frac{1}{\sigma_1} \int_0^d \left( \frac{1}{D_{\pm}^{(1C)}(x)} - 1 \right) dx. \quad (1.17)$$

Here the variable  $x$  occupies the domain  $\xi_N \ll x \ll d - \xi_N$  where the Cooper pair wave functions from the left and right superconductors, see Fig.1.3, do not overlap. At these values of  $x$ , the angle  $\theta(x) \rightarrow 0$ ,  $D_{\pm}(x) \rightarrow 1$  and we can therefore substitute  $x$  by 0 in the integral written in Eq.(1.14).

Taking into account that  $I_{\pm}^{(1C)}(\varepsilon + u) = I_e(\varepsilon) \pm I_h(\varepsilon + 2u)$  we finally get the following important result:

$$(d - x) I_e(\varepsilon) = \sigma_1 [\bar{n}_e^{(1C)}(d) - n_e^{(1C)}(x)], \quad (1.18)$$

where

$$\bar{n}_e^{(1C)}(d) = n_e^{(1C)}(d) - I_e(\varepsilon) m_e^{(1C)}(\varepsilon + u) - I_h(\varepsilon + 2u) m_h^{(1C)}(\varepsilon + u). \quad (1.19)$$

Here  $m_{e(h)}^{(1C)} = [m_+^{(1C)} \pm m_-^{(1C)}]/2$ .

Applying the procedure, Eqs.(1.14)–(1.19), to the left NS interface in Fig.1.3, we find for  $\xi_N \ll x \ll d - \xi_N$ :

$$x I_e(\varepsilon) = \sigma_1 [n_e^{(1L)}(x) - \bar{n}_e^{(1L)}(x = 0)], \quad (1.20)$$

where

$$\begin{aligned} \bar{n}_e^{(1L)}(x = 0) = n_e^{(1L)}(x = 0) + I_e(\varepsilon) m_e^{(1L)}(\varepsilon + u') + \\ I_h(\varepsilon + 2u') m_h^{(1L)}(\varepsilon + u'). \end{aligned} \quad (1.21)$$

Here  $m_{e(h)}^{(1L)} = [m_+^{(1L)} \pm m_-^{(1L)}]/2$ ,

$$m_{\pm}^{(1L)} = \frac{1}{\sigma_1} \int_0^d \left( \frac{1}{D_{\pm}^{(1L)}(x)} - 1 \right) dx. \quad (1.22)$$

Eqs.(1.18)–(1.20) show how  $n_e^{(1)}$  depends on  $x$  in the central part of the normal layer in Fig.1.3. Eq.(1.18) must be consistent with Eq.(1.20). The only way to satisfy this condition is the following one:

$$I_e(\varepsilon) = \frac{\bar{n}_e^{(1C)}(d) - \bar{n}_e^{(1L)}(x = 0)}{R_1}, \quad (1.23)$$

where  $R_1 = d/\sigma_1$  is the normal resistance of the N-layer and we used that  $n_e^{(1L)}(x) = n_e^{(1C)}(x)$ . The condition Eq.(1.23) resembles the Ohm law. It allows to relate the distribution functions at  $x = 0$  and  $x = d$ .

Similar condition holds for  $I_h$ :

$$I_h(\varepsilon) = \frac{\bar{n}_h^{(1C)} - \bar{n}_h^{(1L)}}{R_1}, \quad (1.24)$$

where

$$\bar{n}_h^{(1C)} = n_h^{(1C)}(d) - m_h^{(1C)}(\varepsilon - u) I_e(\varepsilon - 2u) - m_e^{(1C)}(\varepsilon - u) I_h(\varepsilon), \quad (1.25)$$

$$\bar{n}_h^{(1L)} = n_h^{(1L)} + m_h^{(1L)}(\varepsilon - u') I_e(\varepsilon - 2u') + m_e^{(1L)}(\varepsilon - u') I_h(\varepsilon). \quad (1.26)$$

The last step is the formulation of the boundary conditions at the NS interfaces in terms of the distribution functions with bars. Using the  $I_\pm$  notations we can rewrite the boundary conditions, Eqs.(1.10)-(1.11), in the compact form

$$I_\pm^{(1C)}(\varepsilon) = \frac{n_\pm^{(C)}(\varepsilon) - n_\pm^{(1C)}(\varepsilon)}{R_\pm^{(1C)}(\varepsilon + u)}. \quad (1.27)$$

Then it follows from Eq.(1.15) that we can write:

$$I_\pm^{(1C)}(\varepsilon + u) = \frac{n_\pm^{(C)} - \bar{n}_\pm^{(1C)}}{\bar{R}_\pm^{(1C)}(\varepsilon + u)}, \quad (1.28)$$

$$\bar{R}_\pm^{(1C)}(\varepsilon) = m_\pm^{(1C)}(\varepsilon) + R_\pm^{(1C)}(\varepsilon). \quad (1.29)$$

The same form has the boundary condition at  $x = 0$ :

$$I_\pm^{(1L)}(\varepsilon + u') = \frac{\bar{n}_\pm^{(1L)} - n_\pm^{(L)}}{\bar{R}_\pm^{(1L)}(\varepsilon + u')}, \quad (1.30)$$

$$\bar{R}_\pm^{(1L)}(\varepsilon) = m_\pm^{(1L)}(\varepsilon) + R_\pm^{(1L)}(\varepsilon). \quad (1.31)$$

It follows that the physical meaning of  $m_\pm$  terms is the proximity effect contribution to the NS interface resistance, see [15].

It is more convenient to work with the boundary conditions for  $I_{e(h)}$  rather than with those for  $I_\pm$ . Then one can use Eqs.(1.10),(1.11) but with  $n_{e(h)}^{(1L)} \rightarrow \bar{n}_{e(h)}^{(1L)}$  and  $R_{Q(P)}^{(1C)} \rightarrow \bar{R}_{Q(P)}^{(1C)}$ , where, for example,  $\bar{R}_{Q(P)}^{(1C)} = 2\bar{R}_-^{(1C)}\bar{R}_+^{(1C)}/[\bar{R}_+^{(1C)} \pm \bar{R}_-^{(1C)}]$ .

## 1.6 Retarded and advanced Greens functions evolution in normal metals and superconductors

Having formulated the boundary conditions for the distribution functions we turn now to advanced and retarded Greens functions behaviors.

Normal layers in experimental SNS junctions and SNS arrays, see Ref. [17, 19], connect with superconductors like it is shown in Figs.1.4. The junctions of this type are usually referred to as “weak-links”. [27, 28] Boundary conditions for retarded and advanced Greens functions, Eq.(1.2), can be simplified in this case: retarded and advanced Greens functions at superconducting sides of NS boundaries can be substituted by Greens function from the

bulk of the superconductors. These “rigid” boundary conditions approximation is reasonable because the magnitude of the current is much smaller than the critical current of the superconductor [this is assumed] and the current entering the superconductor from narrow normal metal wire with the width comparable with the Cooper pair size. There are also other cases when the rigid boundary conditions are correct, for example, if the NS boundary has the small transparency due to, e.g., an insulator layer at the NS interface.

The recipe telling how one should evaluate  $\theta(x)$  in the normal metal near the NS boundary, where the rigid boundary conditions hold, can be taken from e.g. Ref. [15], and we reproduce briefly their result for the completeness. We will write down  $\theta(x)$  near the right NS boundary (see Fig.1.3 ) taking  $u' = 0$ . In the superconductor,  $\theta_s = \text{atanh}(\Delta/\varepsilon)$ , where  $\Delta$  is the gap. The value of  $\theta_N = \theta(x = 0)$  in the normal metal side should be found from the equation:

$$W \sqrt{\frac{i\Delta}{\varepsilon + i/2\tau_\sigma}} \sinh(\theta_N - \theta_s) + 2 \sinh \frac{\theta_N}{2} = 0, \quad (1.32)$$

where  $W = R_\Delta/R_{\text{NS}}$ ,  $R_\Delta = \xi_\Delta/\sigma_N$ , ( $\xi_\Delta = \sqrt{D/\Delta}$ ) is the resistance of the normal metal layer with the width  $\xi_\Delta$ . Here  $\tau_\sigma$  is the pair breaking rate [29] [e.g., induced by electron-phonon or electron-electron interactions] and  $R_{\text{NS}}$  is the normal resistance of the interface. Then the solution for  $\theta(x > 0)$  is the following:

$$\tanh \frac{\theta}{4} = \exp\left(-\frac{x}{\xi_\varepsilon \sqrt{i}}\right) \tanh \frac{\theta_N}{4}, \quad (1.33)$$

where  $\xi_\varepsilon = \sqrt{D/[2(\varepsilon + i/2\tau_\sigma)]}$ . The effective conductances  $\bar{g}_\pm$  should be expressed through  $\theta$  found from Eqs.(1.32)-(1.33).

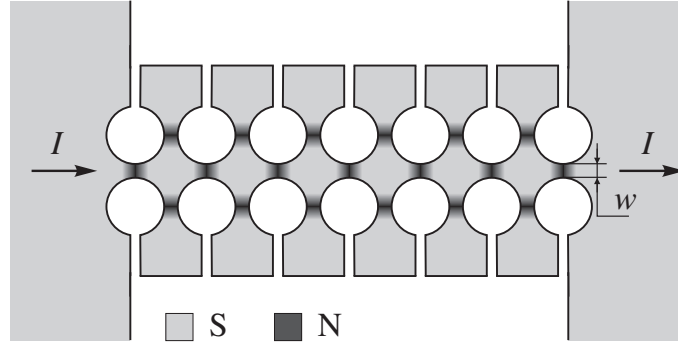


**Fig. 1.4.** Typical experimental array of SNS junctions [17, 19]. This type of the link enables us to use the rigid boundary conditions for the retarded and advanced Greens functions.

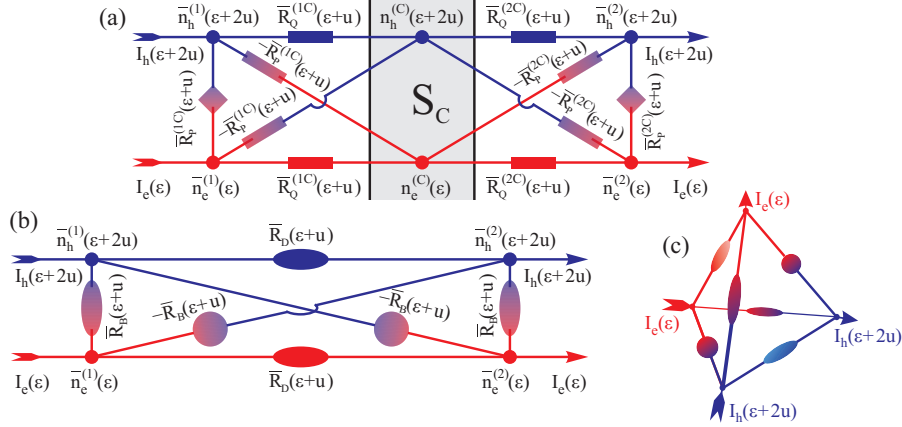


**Fig. 1.5.** (a) Effective circuit representing current conversion at the interfaces of the central superconducting island  $S_C$ . Resistors,  $R_P$  and  $R_Q$  stand for an Andreev- and a normal processes respectively. The role of voltages at the nodes is played by the electron and hole distribution functions. (b) An illustration of the boundary conditions Eqs.(1.34)-(1.36) in terms of a pyramid-circuit is given in this figure. Electron and hole currents entering the left side of the pyramid flow in one normal layer, the right currents flow in the other normal layer. The effective resistance  $\bar{R}_D$  describes the “direct” quasiparticle transmission from one normal layer to the other through the superconductor and the resistance  $\bar{R}_B$  describes Andreev processes. c) Equivalent 3D-sketch of the circuit (b).

## 1.7 Spectral current flow through the superconducting grains

The circuit shown in Fig.1.5a is the graphic representation of the boundary conditions to Eq.(1.2) at the edges of the superconducting island. It is constructed from the circuit units shown in Fig.1.2a. We consider the case where the size of the superconducting island is less than the charge imbalance length, and therefore the coordinate dependence of the quasiparticle distribution functions at the island can be neglected. Solving the Kirchhoff equations for the circuit shown in Fig.1.5a we exclude the quasiparticle distribution functions corresponding to the superconducting island and express the spectral currents through the quasiparticle distribution functions in the normal layers:

$$I_e(\varepsilon) = \frac{\bar{n}_e^{(2)}(\varepsilon) - \bar{n}_e^{(1)}(\varepsilon)}{\bar{R}_D(\varepsilon + u)} + \frac{\bar{n}_h^{(2)}(\varepsilon + 2u) - \bar{n}_h^{(1)}(\varepsilon + 2u)}{\bar{R}_B(\varepsilon + u)}, \quad (1.34)$$

$$I_h(\varepsilon) = \frac{\bar{n}_h^{(2)}(\varepsilon) - \bar{n}_h^{(1)}(\varepsilon)}{\bar{R}_D(\varepsilon - u)} + \frac{\bar{n}_e^{(2)}(\varepsilon - 2u) - \bar{n}_e^{(1)}(\varepsilon - 2u)}{\bar{R}_B(\varepsilon - u)}, \quad (1.35)$$

$$\bar{R}_{D(B)} = 2 \left[ \frac{1}{\bar{R}_+^{(1C)} + \bar{R}_+^{(2C)}} \pm \frac{1}{\bar{R}_-^{(1C)} + \bar{R}_-^{(2C)}} \right]^{-1}. \quad (1.36)$$

The effective resistance  $\bar{R}_D$  describes the “direct” quasiparticle transmission from one normal layer to the other through the superconductor and the resistance  $\bar{R}_B$  describes the Andreev processes, see Fig.1.5b. Note that the direct and indirect transmissions here are different from the so-called “elastic co-tunneling” and “crossed Andreev tunneling” [23, 30] processes where Bogoliubov quasiparticles tunnel below the gap through a thin (with the width of the order of the Cooper pair size) superconducting layer. The probability of these tunneling processes decreases exponentially if the width of the superconducting layer exceeds the Cooper pair size, and they occur without generating supercurrent across a superconductor (the supercurrent flows “virtually”). The size of superconducting islands of the SNS arrays that we consider here exceed well the Cooper pair size, and the current of the quasiparticles with the energies below the gap converts at the NS interface into the supercurrent across the S-islands and then transforms again into the quasiparticle current at the opposite SN-interface.

## 1.8 Recurrent relations

We have demonstrated that there is a direct correspondence between the effective electric circuit and the solution of the Usadel equations with the appropriately chosen boundary conditions. The effective circuit describing transport in SNSNS-array is shown in Fig.1.6. We choose the direction of the current flow in such a way that the electron,  $I_e$ , and the hole,  $I_h$ , currents go in opposite directions. The expression for the total current then assumes the form:

$$\mathcal{I}(V) = -\frac{1}{2e} \int d\varepsilon (I_e + I_h). \quad (1.37)$$

The spectral currents  $I_e$  and  $I_h$  satisfy in general the relation:  $I_e(\varepsilon) = -I_h(\varepsilon)|_{V \rightarrow -V}$ . Similarly,  $n_e(\varepsilon) = n_h(\varepsilon)|_{V \rightarrow -V}$ , ensuring the identity  $\mathcal{I}(-V) = -\mathcal{I}(V)$ .

Writing down the Kirchofs equations for potential distribution at the circuit in Fig. 1.6 we arrive at the recurrent relations, see Appendix A:

$$\begin{aligned} \mathcal{R}(\varepsilon, -u, -V)I_h(\varepsilon) - \rho^{(\circ)}(\varepsilon - u)I_e(\varepsilon - 2u) - \\ \rho^{(\triangleright)}(\varepsilon)I_e(\varepsilon) - \rho^{(\triangleleft)}(\varepsilon - V)I_e(\varepsilon - V) = n_F(\varepsilon) - n_F(\varepsilon - V), \end{aligned} \quad (1.38)$$

$$\begin{aligned} \mathcal{R}(\varepsilon, u, V)I_e(\varepsilon) - \rho^{(\circ)}(\varepsilon + u)I_h(\varepsilon + 2u) - \\ \rho^{(\triangleright)}(\varepsilon)I_h(\varepsilon) - \rho^{(\triangleleft)}(\varepsilon + V)I_h(\varepsilon + 2V) = n_F(\varepsilon + V) - n_F(\varepsilon). \end{aligned} \quad (1.39)$$

Here the effective resistance  $\mathcal{R} = R_1 + R_2 + \rho^{(\triangleright \circ \triangleleft)}$ , where

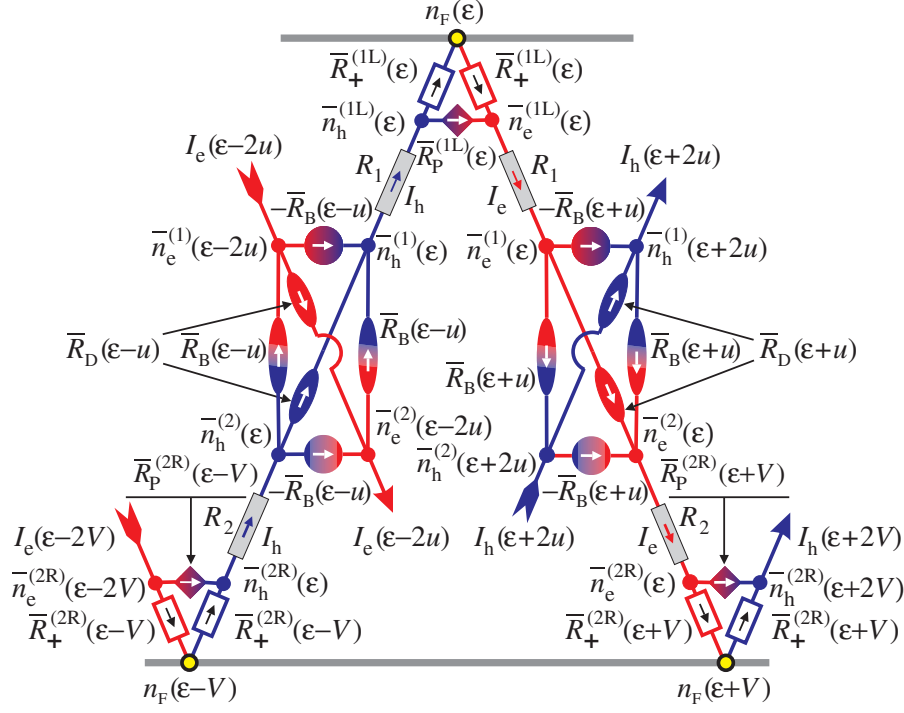


**Fig. 1.6.** MAR in a SNSNS array. The graph shows the effective circuit for quasi-particle currents  $I_e$  and  $I_h$  in the energy space. The role of voltages here play quasi-particle distribution functions. Boxes, triangles and ovals play the role of effective resistances that come from Usadel equations and their boundary conditions.

$$\rho^{(\triangleright \circ \triangleleft)} = (1/2) \sum_{\alpha=\pm} \{ \bar{R}_{\alpha,\epsilon}^{(1L)} + \bar{R}_{\alpha,\epsilon+u}^{(1C)} + \bar{R}_{\alpha,\epsilon+u}^{(2C)} + \bar{R}_{\alpha,\epsilon+V}^{(2R)} \}, \quad (1.40)$$

$$\rho^{(\circ)} = (1/2) \{ \bar{R}_+^{(1C)} + \bar{R}_+^{(2C)} - \bar{R}_-^{(1C)} - \bar{R}_-^{(2C)} \}, \quad (1.41)$$

$$\rho^{(\triangleleft)} = (1/2) \{ \bar{R}_+^{(2R)} - \bar{R}_-^{(2R)} \}, \quad (1.42)$$

$$\rho^{(\triangleright)} = (1/2) \{ \bar{R}_+^{(1L)} - \bar{R}_-^{(1L)} \}. \quad (1.43)$$

In the normal state of the array (or if  $|\epsilon| \gg \Delta$ )  $\mathcal{R}$  reduces to a normal resistance of the array whereas  $\rho^{(\triangleleft)}$  and  $\rho^{(\triangleright)}$  vanish. Then we find from Eqs.(1.38)-(1.39) that  $I_h(\epsilon) = [n_F(\epsilon) - n_F(\epsilon - V)]/\mathcal{R}$ , and  $I_e(\epsilon) = [n_F(\epsilon + V) - n_F(\epsilon)]/\mathcal{R}$  that with Eq.(1.37) reproduces the Ohm's law,  $\mathcal{I} = V/\mathcal{R}$ .

It is easy to find the island potential in the case of symmetrical array when the transmitivities of the island-normal metal interfaces are equal as well as the transmitivities of the lead-normal metal interfaces and  $R_1 = R_2$ . Then the resistances  $\bar{R}_\pm^{(1L)} = \bar{R}_\pm^{(1R)}$ ,  $\bar{R}_\pm^{(1C)} = \bar{R}_\pm^{(2C)}$  and for the symmetry reasons,  $u = V/2$ . At the same time the recurrent relations Eqs.(1.38)-(1.39) become

invariant under the substitution  $I_e(\varepsilon - V) = I_h(\varepsilon)$  and reduce to the relation:

$$\mathcal{R}(\varepsilon, V)I_e(\varepsilon) - \rho^{(\text{p})}(\varepsilon)I_e(\varepsilon - V) - \rho^{(\text{q})}(\varepsilon + V)I_e(\varepsilon + V) = n_F(\varepsilon + V) - n_F(\varepsilon), \quad (1.44)$$

where

$$\begin{aligned} \mathcal{R}(\varepsilon, V) &\equiv \mathcal{R}(\varepsilon, V/2, V) - \rho^{(\text{o})}(\varepsilon + V/2) = \\ &= R_N(\varepsilon) + (1/2) \sum_{\alpha=\pm} \{\bar{R}_{\alpha, \varepsilon}^{(1\text{L})} + \bar{R}_{\alpha, \varepsilon+V}^{(2\text{R})}\}, \end{aligned} \quad (1.45)$$

where  $R_N(\varepsilon) = R_1 + R_2 + \bar{R}_{-, \varepsilon+V/2}^{(1\text{C})} + \bar{R}_{-, \varepsilon+V/2}^{(2\text{C})}$ .

The recurrent relation, Eq.(1.44), is similar to that of a (symmetric) SNS junction, see Ref. [15, 22] and Appendix B, but in our case the normal resistance  $R_N(\varepsilon)$  becomes energy dependent [22]. In other words, a symmetric SNSNS array has the same transport properties as a single (symmetric!) SNS junction, but with the energy dependent resistance of the normal layer. The imbalance resistance  $\bar{R}_{-, \varepsilon}^{(1\text{C})}$  has singularities at the energy corresponding to the gap edges of the superconducting island in the center of our SNSNS array. This is the origin of the subharmonic singularities in the current-voltage characteristics at voltages  $2\Delta/V = n/2$ ,  $n = 1, 2, \dots$ , contrasting the “conventional values” in an SNS junction determined by the relations  $2\Delta/V = n$ . It follows from Eq.(1.45) the unusual subharmonic singularities should disappear if the resistance of the normal layer greatly exceeds the resistance of the SN interfaces. Then  $R_1 \gg \bar{R}_{-, \varepsilon+V/2}^{(1\text{C})} + \bar{R}_{-, \varepsilon+V/2}^{(2\text{C})}$  and the central superconducting island of the SNSNS array effectively “disappears” and the array completely transforms into a SNS junction [22].

## 1.9 Results and Discussion

Calculation of the current-voltage characteristics  $\mathcal{I}(V)$  requires numerical solving of the recurrent relations, Eqs. (1.38)-(1.39). To accomplish the numerical task, we have developed a computational scheme allowing to bypass instabilities caused by the non-analytic behavior of the spectral currents  $I_{e(h)}(\varepsilon)$ , which poses the major computational challenge. The procedure is as follows: first, we fix certain chosen energy  $\varepsilon$  and identify the set of energies connected through the equations in the given energy interval, solving afterwards the resulting subsystem of equations. We then repeat the procedure, until the required energy resolution of  $\delta\varepsilon = 10^{-5}\Delta$  is achieved. Typically, up to  $10^6$  linear equations had to be solved for every given voltage, but the complexity of the coupled subsystem depends on the commensurability of  $u$  and  $V$ .

Figure 1.7 shows the comparative results for the SNSNS junction and two SNS junctions in series. The latter corresponds to the case where the size of the central island well exceeds the energy relaxation length,  $L_C > \ell_\varepsilon$ .

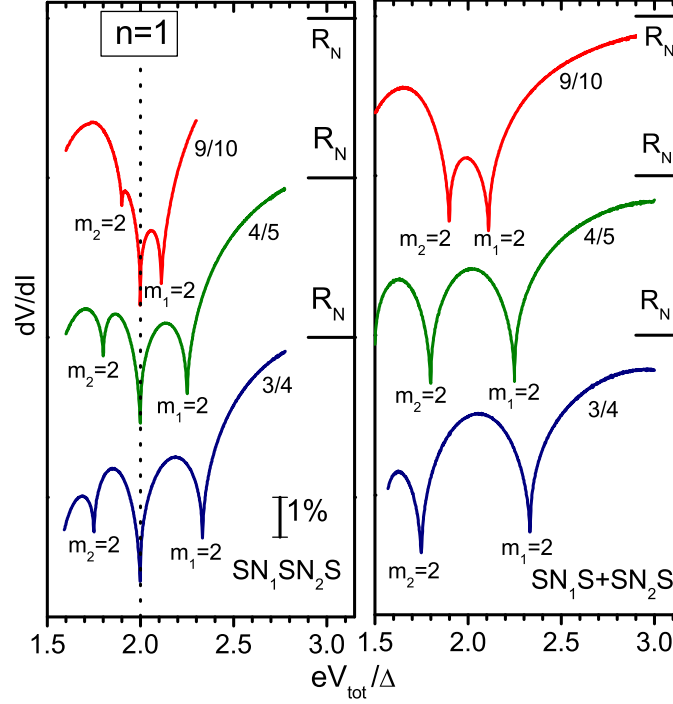


**Fig. 1.7.** Left panel: Differential resistances as functions of the applied voltage  $V_{\text{tot}}$  (around  $n = 1$  in Eq. (1)) for the  $\text{SN}_1\text{SN}_2\text{S}$  junction. The fractions  $3/4$ , and  $4/5$ , and  $9/10$  represent the ratios of resistances of the normal regions,  $R_1/R_2$ . The differential resistance  $dV/dI$  of the  $\text{SN}_1\text{SN}_2\text{S}$  junction demonstrates the pronounced SAT spike at  $V_{\text{tot}} = 2\Delta/e$ , irrespectively to the partial voltage drops. The SAT spike is sandwiched between the two additional spikes corresponding to individual MAR processes occurring at junctions  $\text{SN}_1\text{S}$  and  $\text{SN}_2\text{S}$  for  $m_1, m_2 = 2$ . The voltage positions of these features depend on  $R_1/R_2$ . Right panel: The corresponding  $dV/dI(V_1 + V_2)$  for the two  $\text{SN}_1\text{S}$  and  $\text{SN}_2\text{S}$  junctions in series as they would have appeared in the absence of the synchronization process, i.e. in the case where  $L_C > \ell_\epsilon$ . These  $dV/dI$  dependencies were calculated following [15] (with transmissivity  $W=1$ ).

We display the differential resistances as functions of the applied voltage, which demonstrate the singularities in Andreev transmission more profoundly than the  $I$ - $V$  curves. There is a pronounced SAT spike in the  $dV/dI$  for an SNSNS junction at  $V_{\text{tot}} = 2\Delta/e$ . The spike appears irrespectively to the partial voltage drops in the normal regions and is absent in the corresponding curves representing two individual MAR processes at the junctions  $\text{SN}_1\text{S}$  and  $\text{SN}_2\text{S}$ .

The resonant voltages of the SAT singularities can be found from the consideration of the quasiparticle trajectories in the space-energy diagrams.



Such a diagram for the first subharmonic,  $n = 1$  and ratio  $R_1/R_2 = 3/4$  is given in Fig. 1.1. A quasiparticle starts from the left superconducting electrode with the energy  $\varepsilon = -\Delta$  to traverse  $N_1$ , and the quasiparticle that starts from the central island  $S_c$  with the same energy as the incident one to take up upon the current across the island  $N_2$ , and hit  $S_R$  with the energy  $\varepsilon = \Delta$  (the ABCD path, the corresponding path for the hole is D'C'B'A'). In general, relevant trajectories yielding resonant voltages of Eq. (1.1) have the following structure: they start and end at the BCS quasiparticle density of states singular points ( $\varepsilon = \pm\Delta$ ), contain the closed polygonal path, which include MAR staircases in the normal parts and over-the-gap transmissions and Andreev reflections, and pass the density of states singular points at the central island. Apart from the main singularities [Eq. (1.1)], additional SAT satellite spikes appear at  $V = (2\Delta/e)(p+q)/n$ , where  $p/q$  is the irreducible rational approximation of the real number  $r = R_1/R_2$ , (we take  $R_1 < R_2$ ), and  $n \geq (p+q)$ .

The achieved qualitative understanding enables us to observe that the manifestations of the SAT mechanism in an experimental situation becomes even more pronounced with the growth of the number of SNS junctions in the system. To see this, let us assume that the resistances of the normal islands in a chain of SNS junctions are randomly scattered around their average value  $R_0$  and follow Gaussian statistics with the standard deviation  $\sigma_R = \sigma R_0$ , where  $\sigma$  is dimensionless. Accordingly, the dispersion of the distribution of the MAR resonant voltages is characterized by the same  $\sigma$ , and the MAR features get smeared. Let us distribute the voltage drop  $2\Delta/e$  among the  $n$  successive islands. Then the quasiparticle SAT path starts at the lower edge of the superconducting gap at island  $j$ , traverses  $n-1$  intermediate superconducting islands and hits the edge of the gap at the  $j+n$ -th island in the chain. The standard deviation of the voltage drop on the  $n$  islands grows as  $\sqrt{n}$  resulting in a voltage deviation per one island  $\propto 1/\sqrt{n}$ , i.e. the dispersion of the distribution of  $V_n$  drops with increasing  $n$ :  $\sigma_{SAT} = \sigma/\sqrt{n}$ . In contrast to the MAR-induced features, with an increase of  $n$ , the subharmonic spikes at voltages  $V_n$  per junction due to SAT processes become more sharp and pronounced.

## 1.10 Conclusions

In conclusion, we have developed a nonequilibrium theory of the charge transfer across a central superconducting island in an SNSNS array and found that this island acts as Andreev *retransmitter*. We have shown that the nonequilibrium transport through an SNSNS array is governed by the synchronized Andreev transmission with the correlated conversion processes at the opposite NS interfaces of the central island. The constructed theory is a fundamental building unit for a general quantitative description of a large array consisting of many SNS junctions.

### 1.11 Acknowledgments

We thank A. N. Omelyanchuk for helpful discussions. The work was supported by the U.S. Department of Energy Office of Science under the Contract No. DE-AC02-06CH11357, and partially by the RFBR 10-02-00700, Russian President Science Support foundation mk-7674.2010.2, the Dynasty, Russian Federal Programs and the Programs of the Russian Academy of Science.

## A Recurrent relations for the quasiparticle currents and distribution functions

The Kirchhoff's laws applied for the circuit in Fig. 1.6 generate the following linear system of equations:

$$I_e(\varepsilon - 2V) = \frac{\bar{n}_{h,\varepsilon}^{(2R)} - \bar{n}_{e,\varepsilon-2V}^{(2R)}}{\bar{R}_{P,\varepsilon-V}^{(2R)}} + \frac{n_F(\varepsilon - V) - \bar{n}_{e,\varepsilon-2V}^{(2R)}}{\bar{R}_{+,\varepsilon}^{(2R)}}, \quad (1.46)$$

$$I_h(\varepsilon) = \frac{\bar{n}_h^{(2R)} - \bar{n}_{e,\varepsilon-2V}^{(2R)}}{\bar{R}_{P,\varepsilon-V}^{(2R)}} + \frac{\bar{n}_h^{(4)} - n_F(\varepsilon - V)}{\bar{R}_{+,\varepsilon-V}^{(2R)}}, \quad (1.47)$$

$$I_h(\varepsilon) = \frac{\bar{n}_h^{(2)} - \bar{n}_h^{(2R)}}{R_2}, \quad (1.48)$$

$$I_h(\varepsilon) = \frac{\bar{n}_{h,\varepsilon}^{(1)} - \bar{n}_{h,\varepsilon}^{(2)}}{\bar{R}_{D,\varepsilon-u}} + \frac{\bar{n}_{e,\varepsilon-2u}^{(1)} - \bar{n}_{e,\varepsilon-2u}^{(2)}}{\bar{R}_{B,\varepsilon-u}}, \quad (1.49)$$

$$I_e(\varepsilon - 2u) = \frac{\bar{n}_{e,\varepsilon-2u}^{(2)} - \bar{n}_{e,\varepsilon-2u}^{(1)}}{\bar{R}_{D,\varepsilon-u}} + \frac{\bar{n}_{h,\varepsilon}^{(2)} - \bar{n}_{h,\varepsilon}^{(1)}}{\bar{R}_{B,\varepsilon-u}}, \quad (1.50)$$

$$I_h(\varepsilon) = \frac{\bar{n}_h^{(1L)} - \bar{n}_h^{(1C)}}{R_1} \quad (1.51)$$

$$I_h(\varepsilon) = \frac{\bar{n}_e^{(1L)} - \bar{n}_h^{(1L)}}{\bar{R}_{P,\varepsilon}^{(1L)}} + \frac{n_F(\varepsilon) - \bar{n}_h^{(1L)}}{\bar{R}_{+,\varepsilon}^{(1L)}}, \quad (1.52)$$

and

$$I_h(\varepsilon + 2V) = \frac{\bar{n}_{h,\varepsilon+2V}^{(2R)} - \bar{n}_e^{(2R)}}{\bar{R}_{P,\varepsilon+V}^{(2R)}} + \frac{\bar{n}_{h,\varepsilon+2V}^{(2R)} - n_F(\varepsilon + V)}{\bar{R}_{P,\varepsilon+V}^{(2R)}}, \quad (1.53)$$

$$I_e(\varepsilon) = \frac{\bar{n}_{h,\varepsilon+2V}^{(2R)} - \bar{n}_{e,\varepsilon}^{(2R)}}{\bar{R}_{P,\varepsilon+V}^{(2R)}} + \frac{n_F(\varepsilon + V) - \bar{n}_{e,\varepsilon}^{(2R)}}{\bar{R}_{P,\varepsilon+V}^{(2R)}}, \quad (1.54)$$

$$I_e(\varepsilon) = \frac{\bar{n}_{e,\varepsilon}^{(2R)} - \bar{n}_{e,\varepsilon}^{(2C)}}{R_2}, \quad (1.55)$$

$$I_e(\varepsilon) = \frac{\bar{n}_{e,\varepsilon}^{(2C)} - \bar{n}_{e,\varepsilon}^{(1C)}}{\bar{R}_{D,\varepsilon+u}^{(12)}} + \frac{\bar{n}_{e,\varepsilon+2u}^{(2C)} - \bar{n}_{e,\varepsilon+2u}^{(1C)}}{\bar{R}_{B,\varepsilon+u}^{(12)}}, \quad (1.56)$$

$$I_h(\varepsilon + 2u) = \frac{\bar{n}_{h,\varepsilon+2u}^{(1C)} - \bar{n}_{h,\varepsilon+2u}^{(2C)}}{\bar{R}_{D,\varepsilon+u}^{(12)}} + \frac{\bar{n}_{e,\varepsilon}^{(1C)} - \bar{n}_{e,\varepsilon}^{(2C)}}{\bar{R}_{B,\varepsilon+u}^{(12)}}, \quad (1.57)$$

$$I_e(\varepsilon) = \frac{\bar{n}_{e,\varepsilon}^{(1C)} - \bar{n}_{e,\varepsilon}^{(1L)}}{R_1}, \quad (1.58)$$

$$I_e(\varepsilon) = \frac{\bar{n}_{e,\varepsilon}^{(1L)} - \bar{n}_{h,\varepsilon}^{(1L)}}{\bar{R}_{P,\varepsilon}^{(1L)}} + \frac{\bar{n}_{e,\varepsilon}^{(1L)} - n_F(\varepsilon)}{\bar{R}_{F,\varepsilon}^{(1L)}}. \quad (1.59)$$

Eqs.(1.46)-(1.59) are the recurrent relations (i.e. the relations coupling the functions at energy  $\varepsilon$  with the functions at  $\varepsilon \pm V$ ) for the currents and the distribution functions.

It follows from Eqs.(1.48),(1.51) that

$$I_{h,\varepsilon} [R_1 + R_2] = \bar{n}_h^{(2C)} - \bar{n}_h^{(2R)} + \bar{n}_h^{(1L)} - \bar{n}_h^{(1C)}. \quad (1.60)$$

The distributions functions entering Eq.(1.60) we can express below through the currents. Combining Eqs.(1.49)-(1.50) we get,

$$\bar{n}_h^{(1C)} - \bar{n}_h^{(2C)} = \frac{[I_{h,\varepsilon} \bar{R}_{u,\varepsilon-u} + I_{e,\varepsilon-2u} \bar{R}_{D,\varepsilon-u}] \bar{R}_{D,\varepsilon-u} \bar{R}_{B,\varepsilon-u}}{(\bar{R}_{B,\varepsilon-u})^2 - (\bar{R}_{D,\varepsilon-u})^2}. \quad (1.61)$$

At the same time from Eqs.(1.52),(1.59) follows that

$$\bar{n}_{h,\varepsilon}^{(1L)} = n_F(\varepsilon) + \bar{R}_{+,\varepsilon}^{(1L)} \frac{I_e \bar{R}_{+,\varepsilon}^{(1L)} - I_h (\bar{R}_{P,\varepsilon}^{(1L)} + \bar{R}_{+,\varepsilon}^{(1L)})}{2\bar{R}_{+,\varepsilon}^{(1L)} + \bar{R}_{P,\varepsilon}^{(1L)}}, \quad (1.62)$$

and finally from Eqs.(1.46)-(1.47) we get

$$\bar{n}_{h,\varepsilon}^{(2R)} = n_F(\varepsilon - V) + \bar{R}_{+,\varepsilon-V}^{(2R)} \frac{-I_{e,\varepsilon-2V} \bar{R}_{+,\varepsilon-V}^{(2R)} + I_h (\bar{R}_{+,\varepsilon-V}^{(2R)} + \bar{R}_{P,\varepsilon-V}^{(2R)})}{2\bar{R}_{+,\varepsilon-V}^{(2R)} + \bar{R}_{P,\varepsilon-V}^{(2R)}}. \quad (1.63)$$

Combining Eq.(1.60) and Eqs.(1.61)-(1.63) we find the recurrent relation for the currents, Eq.(1.38). Similar procedure helps to derive Eq.(1.39).

## B Charge transport in SNS junctions

We discuss below the transport properties of SNS and SNN' junctions to make a mapping between our technique and the well-known results obtained before us.

The recurrent relations, Eqs.(1.38)-(1.39), solve the transport problem in a SNS junction in the incoherent regime. Then there is no island, so  $\rho^{(\circ)} = 0$  and we should remove the island resistances with the indices (1C) and (2C) from the coefficient functions of the recurrent relations. So,

$$\mathcal{R}(\varepsilon, -V)I_h(\varepsilon) - \rho^{(\triangleright)}(\varepsilon)I_e(\varepsilon) - \rho^{(\triangleleft)}(\varepsilon - V)I_e(\varepsilon - V) = n_F(\varepsilon) - n_F(\varepsilon - V), \quad (1.64)$$

$$\mathcal{R}(\varepsilon, V)I_e(\varepsilon) - \rho^{(\triangleright)}(\varepsilon)I_h(\varepsilon) - \rho^{(\triangleleft)}(\varepsilon + V)I_h(\varepsilon + 2V) = n_F(\varepsilon + V) - n_F(\varepsilon), \quad (1.65)$$

where, for example,

$$\mathcal{R}(\varepsilon, V) = R_1 + R_2 + (1/2) \sum_{\alpha=\pm} \{ \bar{R}_{\alpha, \varepsilon}^{(1L)} + \bar{R}_{\alpha, \varepsilon+V}^{(2R)} \}. \quad (1.66)$$

Eqs.(1.64)-(1.65) are invariant under the following transformation,  $I_e(\varepsilon - V) \rightarrow I_h(\varepsilon)$ , if *at the same time* we exchange the resistances,  $\bar{R}_{\pm, \varepsilon}^{(1L)} \leftrightarrow \bar{R}_{\pm, \varepsilon}^{(1R)}$ . Thus the relation,  $I_e(\varepsilon - V) = I_h(\varepsilon)$  and the reduction of the recurrent relations to the one equation for  $I_e$  or for  $I_h$  as it was done in Ref. [15]:

$$\mathcal{R}(\varepsilon, V)I_e(\varepsilon) - \rho^{(\triangleright)}(\varepsilon)I_e(\varepsilon - V) - \rho^{(\triangleleft)}(\varepsilon + V)I_e(\varepsilon + V) = n_F(\varepsilon + V) - n_F(\varepsilon), \quad (1.67)$$

holds only for a *symmetric* SNS junction with  $\bar{R}_{\pm, \varepsilon}^{(1L)} = \bar{R}_{\pm, \varepsilon}^{(1R)}$ .

To summarize here our consideration [summarized by the recurrent relations Eqs.(1.64)-(1.65)], reduces to that presented in Ref. [15] only in the case where the contacts are symmetric and the assumption  $I_e(\varepsilon - V) = I_h(\varepsilon)$  holds.

## References

1. A. F. Andreev, Zh. Eksp. Teor. Fiz. **46** (1964) 1823 [Sov. Phys. JETP **19** (1964) 1228].
2. J. M. Rowell and W. E. Feldmann, Phys. Rev. **172**, 393 (1968).
3. P. E. Gregers-Hansen, E. Hendricks, M. T. Levinsen, and G. R. Pickett, Phys. Rev. Lett. **31**, 524 (1973).
4. W. M. van Hufelen, T. M. Klapwijk, D. R. Heslinga, M. J. de Boer, and N. van der Post, Phys. Rev. B **47**, 5170 (1993).
5. A. W. Kleinsasser, R. E. Miller, W. H. Mallison, and G. B. Arnold, Phys. Rev. Lett. **72**, 1738 (1994).

6. E. Scheer, P. Joyez, D. Esteve, C. Urbina, and M. H. Devoret, Phys. Rev. Lett. **78**, 3535 (1997).
7. J. Kutchinsky, R. Taboryski, T. Clausen, C. B. Sørensen, A. Kristensen, P. E. Lindelof, J. Bindslev Hansen, C. Schelde Jacobsen, and J. L. Skov, Phys. Rev. Lett. **78**, 931 (1997).
8. A. Frydman and R. C. Dynes, Phys. Rev. B **59**, 8432 (1999).
9. T. Hoss, C. Strunk, T. Nussbaumer, R. Huber, U. Staufer, and C. Schönenberger, Phys. Rev. B **62**, 4079 (2000).
10. T. I. Baturina, Z. D. Kvon, R. A. Donaton, M. R. Baklanov, E. B. Olshanetsky, K. Maex, A. E. Plotnikov, J. C. Portal, Physica B **284**, 1860 (2000).
11. Z. D. Kvon, T. I. Baturina, R. A. Donaton, M. R. Baklanov, K. Maex, E. B. Olshanetsky, A. E. Plotnikov, J. C. Portal, Phys. Rev. B **61**, 11340 (2000).
12. T. M. Klapwijk, G. E. Blonder, and M. Tinkham, Physica B+C (Amsterdam) **110**, 1657 (1982).
13. M. Octavio, M. Tinkham, G. E. Blonder, and T. M. Klapwijk, Phys. Rev. B **27**, 6739 (1983).
14. K. Flensberg, J. Bindslev Hansen, and M. Octavio, Phys. Rev. B **38**, 8707 (1988).
15. E. V. Bezuglyi, E. N. Bratus', V. S. Shumeiko, G. Wendin, H. Takayanagi, Phys. Rev. B **62**, 14439 (2000). In this work superconductors were considered to be in a local equilibrium and the relation  $I_e(\varepsilon) = I_h(\varepsilon - V)$  was satisfied. This approach was further developed by N. M. Chtchelkatchev, [22]; however in case of geometrically non-symmetric SNS arrays, it results in an equivalent circuit with the enumerable number of elements.
16. J. C. Cuevas, J. Hammer, J. Kopu, J. K. Viljas, and M. Eschrig, Phys. Rev. B **73**, 184505 (2006).
17. T. I. Baturina, Z. D. Kvon, and A. E. Plotnikov, Phys. Rev. B **63**, 180503(R) (2001).
18. T. I. Baturina, Yu. A. Tsaplin, A. E. Plotnikov, and M. R. Baklanov, JETP Lett. **81**, 10 (2005).
19. T. I. Baturina, D. R. Islamov, and Z. D. Kvon, JETP Lett. **75**, 326 (2002).
20. J. Fritzsche, R. B. G. Kramer, and V. V. Moshchalkov, Phys. Rev. B **80**, 094514 (2009).
21. T. I. Baturina, A. Yu. Mironov, V. M. Vinokur, N. M. Chtchelkatchev, A. Glatz, D. A. Nasimov, A. V. Latyshev, Physica C (2009) doi:10.1016/j.physc.2009.11.107
22. N. M. Chtchelkatchev, JETP Lett. **83**, 250 (2005).
23. G. Deutscher and D. Feinberg, Appl. Phys. Lett. **76**, 487 (2000).
24. A. I. Larkin and Yu. N. Ovchinnikov, Sov. Phys. JETP **41**, 960 (1975); *ibid*, **46**, 155 (1977).
25. M. Yu. Kupriyanov and V. F. Lukichev, Zh. Eksp. Teor. Fiz. **94**, 139 (1988) [Sov. Phys. JETP **67**, 1163 (1988)].
26. A. F. Volkov and T. M. Klapwijk, Phys. Lett. A **168**, 217 (1992).
27. K. K. Likharev, Rev. Mod. Phys. **51**, 101 (1979).
28. C. W. J. Beenakker, Phys. Rev. Lett. **67**, 3836 (1991).
29. M. Tinkham, Introduction to superconductivity, Mc.Graw-Hill Inc., 1996.
30. N. M. Chtchelkatchev, JETP Lett. **78**, 230 (2003).

